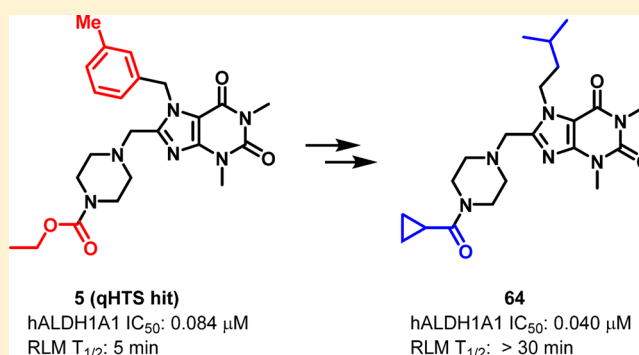


Discovery of NCT-501, a Potent and Selective Theophylline-Based Inhibitor of Aldehyde Dehydrogenase 1A1 (ALDH1A1)

Shyh-Ming Yang,^{*,†} Adam Yasgar,[†] Bettina Miller,[‡] Madhu Lal-Nag,[†] Kyle Brimacombe,[†] Xin Hu,[†] Hongmao Sun,[†] Amy Wang,[†] Xin Xu,[†] Kimloan Nguyen,[†] Udo Oppermann,^{§,||} Marc Ferrer,[†] Vasilis Vasiliou,^{‡,⊥} Anton Simeonov,[†] Ajit Jadhav,[†] and David J. Maloney^{*,†}[†]National Center for Advancing Translational Sciences, National Institutes of Health, 9800 Medical Center Drive, Rockville, Maryland 20850, United States[‡]Department of Pharmaceutical Sciences, Skaggs School of Pharmacy and Pharmaceutical Sciences, University of Colorado Anschutz Medical Campus, Aurora, Colorado 80045, United States[§]Botnar Research Center, NIHR Oxford Biomedical Research Unit, Oxford OX3 7LD, U.K.^{||}Structural Genomics Consortium, University of Oxford, Old Road Campus, Roosevelt Drive, Oxford OX3 7DQ, U.K.[⊥]Department of Environmental Health Sciences, Yale School of Public Health, 60 College Street, New Haven, Connecticut 06510, United States

Supporting Information

ABSTRACT: Aldehyde dehydrogenases (ALDHs) metabolize reactive aldehydes and possess important physiological and toxicological functions in areas such as CNS, metabolic disorders, and cancers. Increased ALDH (e.g., ALDH1A1) gene expression and catalytic activity are vital biomarkers in a number of malignancies and cancer stem cells, highlighting the need for the identification and development of small molecule ALDH inhibitors. A new series of theophylline-based analogs as potent ALDH1A1 inhibitors is described. The optimization of hits identified from a quantitative high throughput screening (qHTS) campaign led to analogs with improved potency and early ADME properties. This chemotype exhibits highly selective inhibition against ALDH1A1 over ALDH3A1, ALDH1B1, and ALDH2 isozymes as well as other dehydrogenases such as HPGD and HSD17β4. Moreover, the pharmacokinetic evaluation of selected analog **64** (NCT-501) is also highlighted.



INTRODUCTION

The human genome encodes 19 aldehyde dehydrogenase (ALDH) enzymes that metabolize reactive aldehydes to their corresponding carboxylic acid derivatives.¹ Unbalanced biological activity of ALDHs and specific contribution to their metabolism pathway have been associated in a variety of disease states, including alcoholic liver disease, Sjögren–Larsson syndrome (SLS), type 2 hyperprolinemia, hyperammonemia, Parkinson's disease, and cancers.^{2–5} It is well established that overexpression of certain ALDHs, especially ALDH1A1, in a number of malignancies and cancer stem cells (CSCs) correlates with poor prognosis and tumor aggressiveness and that ALDH1A1 is linked to drug resistance in traditional cancer chemotherapy.^{6,7} Although the majority of the research community has considered ALDH1A1 as a marker of cancer stem cells and a predictor of the prognosis, this enzyme also plays an important role in the biology of tumors and cancer stem cells.^{8,9} Initial evidence toward this end has been established using nonspecific ALDH inhibitors and siRNA silencing techniques.¹⁰ More recently, ALDH1A1 has also been

implicated in obesity^{11,12} and inflammation,¹³ suggesting that inhibition of this enzyme may offer new therapeutic options for obese patients and patients with Crohn's disease.¹³ These data suggest that discovery of small molecule ALDH inhibitors is a prudent approach for identifying potential cancer and/or CSC-directed therapeutics as well as a better understanding of the physiological and pathophysiological actions of the ALDHs.^{14,15}

Among reported ALDH inhibitors,¹⁶ CVT-10216 (**1**) represents an attractive small molecule that effectively inhibits both ALDH1A (1.3 μM) and ALDH2 (0.029 μM) (Figure 1).¹⁷ This reversible inhibitor was designed and optimized based on the interaction of daidzin (**2**) with human ALDH2.^{18,19} As a result of the potent ALDH2 inhibition, **1** has been developed for the treatment of alcoholism and has also demonstrated activity in the reduction of cocaine-seeking behavior.²⁰ More recently, indolinedione-based analogs (e.g., **3**)²¹ and substituted tricyclic pyrimidinone **4**²² reported by

Received: April 13, 2015

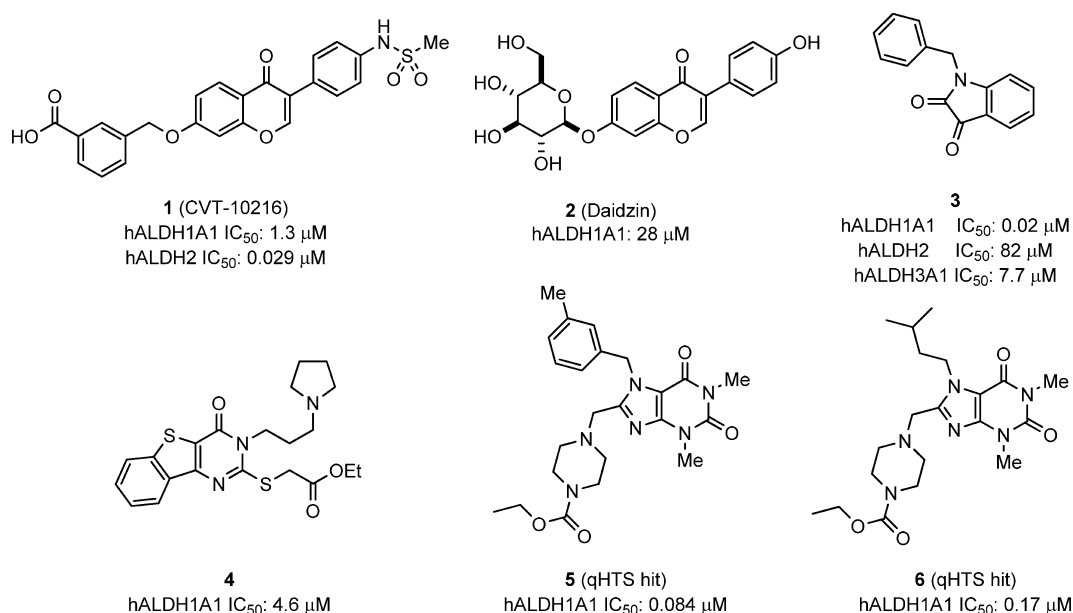


Figure 1. Representative small molecule ALDH1A1 inhibitors and theophylline-based qHTS hits.

Hurley and co-workers exhibit significant hALDH1A1 inhibitory activity (0.02 and 4.6 μM for 3 and 4, respectively) and were reported to be selective inhibitors against other ALDH isozymes such as ADLH2 and ALDH3A1. The 3-carbonyl functionality of these indolinedione analogs appears to form reversible covalent adducts with catalytic cysteine residue, particularly with ALDH3A1, and additional mechanism of action studies suggest that these molecules are substrate competitive inhibitors.^{21,22} Furthermore, the inhibition of ALDH1A1 activity by compound 4 resulted in disruption of ovarian cancer spheroid formation and cell viability. Despite the favorable activity of these compounds, to the best of our knowledge a systematic and thorough medicinal chemistry effort had not been reported on ALDH1A1 inhibitors. As such, our efforts toward identifying novel, more druglike small molecule of ALDH1A1 inhibitors for cancer and CSCs research began with a qHTS²³ campaign (PubChem assay identifier 1030: <http://pubchem.ncbi.nlm.nih.gov/assay/assay.cgi?aid=1030>, last modified March 15, 2010) that ultimately led to identification of the theophylline-based chemotype, exemplified as hits 5 (0.084 μM) and 6 (0.17 μM), along with other active analogs (Figure 1).^{24,25} Furthermore, we aimed to fill the need for optimized druglike ALDH1A1 inhibitors with improved ADME/PK properties required for evaluating the fundamental biological roles (e.g., cancer and CSCs) of ALDH1A1 in vivo. These theophylline-based hits (e.g., 5 and 6) are structurally distinct from existing ALDH inhibitors and appear quite specific with minimal activity across 570 assays screened in PubChem, which suggests the theophylline core is a suitable scaffold for further investigation.^{26,27} Herein, we report the systematic medicinal chemistry optimization and structure–activity relationships (SARs) of the theophylline-based analogs as potent and selective ALDH1A1 inhibitors.

CHEMISTRY

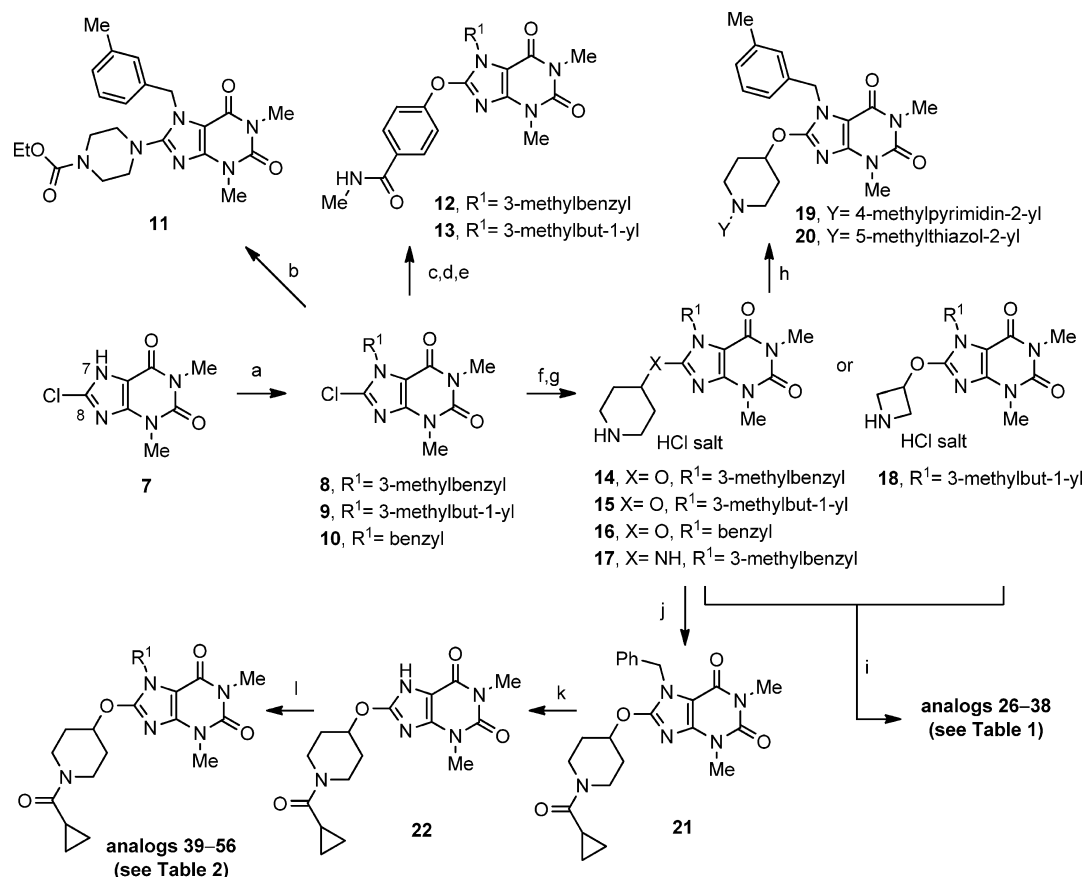
The synthetic routes that allow access to the majority of designed molecules with modification of two arms (N7 and C8) of theophylline core are described in Scheme 1.²⁸ Alkylation of commercially available 8-chlorotheophylline 7

with representative bromides provided intermediates 8–10 in which the Cl functionality is poised for derivatization of the C8 substitution. For instance, analog 11 was readily prepared by utilizing a substitution protocol with ethoxycarbonylpiperazine under microwave irradiation. Analogs 12–13 were synthesized similarly by Cl displacement with methyl 4-hydroxybenzoate followed by hydrolysis and methyl amide formation. The key intermediates 14–18 with diverse C8 substitutions that focused on the variation of ring size (four-membered vs six-membered rings) and linkers (O or NH) were generated in a similar manner after Boc deprotection. With these intermediates in hand, the piperidine moiety was further reacted with halo-substituted heteroarenes to give 19 and 20, acylated or sulfonated with substituted carbonyl chloride or sulfonyl chloride, respectively, to furnish analogs 26–38 (see Table 1). These transformations allowed for efficient SAR investigations around ethyl carbamate portion of qHTS hits. Further utilizing intermediate 16 by acylation with cyclopropanecarbonyl chloride followed by removal of the benzyl group under palladium-catalyzed hydrogenation conditions gave intermediate 22. This is then poised for derivatization of the N7 position by alkylation or a Mitsunobu reaction with the requisite halides or hydroxyl material, respectively, to provide analogs 39–56 (see Table 2).

The piperazine-type analogs, including resynthesized hits 5 and 6, were prepared in a different manner as highlighted in Scheme 2. The hydroxyl intermediate 24 was generated via a two-step sequence involving acylation of 23 with hydroxyacetic acid followed by cyclization under basic conditions.²⁹ Further alkylation with various alkyl and benzyl bromides followed by oxidation with Dess–Martin periodinane gave aldehyde 25. Subsequent reductive amination with corresponding piperazine derivatives using sodium triacetoxyborohydride as the reducing agent afforded qHTS hits 5 and 6 and desired analogs 57–67 (see Table 3).

RESULTS AND DISCUSSION

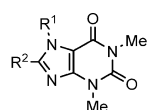
Structure–Activity Relationships (SARs). The inhibitory activity of these analogs was tested using human ALDH1A1

Scheme 1. Synthetic Routes Assessing Theophylline-Based ALDH1A1 Inhibitors^a

^aReagents and conditions: (a) R¹-Br, K₂CO₃, DMF, rt to 60 °C, 1–24 h, **8** (98%), **9** (95%), **10** (99%); (b) 1-ethoxycarbonylpiperazine, DMSO, microwave, 160 °C, 30 min, **11** (58%); (c) methyl 4-hydroxybenzoate, K₂CO₃, DMF, microwave, 160 °C, 1 h, 66–83%; (d) 1.5 N LiOH_(aq), THF/MeOH, 50 °C, 2–3 h, 48–70%; (e) MeNH₂ (2 M in THF), HATU, DMF, (*i*-Pr)₂NEt, rt, 2 h, 46–59%; (f) *N*-Boc-4-hydroxyazetidone (for **14–16** and **18**), NaH, DMF, rt, 0.5–2 h, 81–96%; or *N*-Boc-4-aminopiperidine (for **17**), DMSO, microwave, 160 °C, 45 min, 66%; (g) 4 M HCl in dioxane, rt, 3–24 h, 90–99%; (h) 2-chloro-4-methylpyrimidine or 2-bromo-5-methylthiazole, K₂CO₃, DMF, microwave, 160 °C, 1 h; (i) corresponding substituted carbonyl chloride, Et₃N, CH₂Cl₂, rt, 0.5–1 h, for **26–27**, **29–34**, and **36–38**; or ethyl isocyanate, Et₃N, CH₂Cl₂, rt, 0.5 h, for **28**; or cyclopropanesulfonyl chloride, Et₃N, CH₂Cl₂, rt, 0.5 h, for **35**; (j) **16**, cyclopropanecarbonyl chloride, Et₃N, CH₂Cl₂, rt, 0.5 h, **21** (96%); (k) Pd(OH)₂ (20 mol %), EtOAc/EtOH, 70 °C, 24 h, **22** (75%); (l) corresponding alkyl or benzyl bromide or chloride, K₂CO₃, DMF, 50–60 °C, 3–24 h, for **39–52**; or corresponding hydroxyl compounds, ^tBuO₂CN=NCO₂^tBu, PPh₃, THF, rt or 60 °C, 1–3 h, for **53–56**.

(hALDH1A1). Importantly, the resynthesized material of **5** and **6** had comparable potency to that obtained in the primary qHTS assay (Table 1). As part of our medicinal chemistry optimization campaign, we also characterized all synthesized compounds for early ADME (eADME) data such as microsomal stability, PAMPA permeability, and aqueous solubility (pH 7.4) to concurrently develop structure–property relationships. Thus, we immediately realized that our hit compounds possessed poor rat liver microsomal (RLM) stability (**5**, $t_{1/2}$ = 5 min) which would need to be improved along with retaining the desired potency and selectivity profile. Initial structural modifications were primarily focused on the R² portion as shown in Table 1. With the 3-methylbenzyl R¹ substitution held constant, direct attachment of the piperazine substituent (**11**) or rearranging the nitrogen atom from piperazine to aminopiperidine substituent (**26**) resulted in ~14-fold loss of potency. While the hydroxypiperidine analog exhibited reasonable inhibitory activity (**27**, 213 nM), removal of the ethyl carbamate functionality significantly dropped the potency to the micromolar range (**14**, 13.7 μM), indicating further investigation of this position was required. Subsequently, changing the ethyl carbamate to ethylurea (**28**) or short

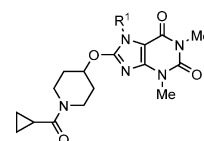
chain amides (**29** and **30**) minimally affected the potency. However, increasing the size of side chain, such as **31** and **32**, resulted in a loss of potency. In comparison with linear amides such as **31**, the branched amides (e.g., **33** and **34**), particularly cyclopropylamide, showed significant improvement in potency (**34**, 84 nM). Switching the cyclopropylamide to sulfonamide (**35**) caused a 3-fold potency loss. Other attempts to structurally mimic ethyl carbamate with simple methylheteroarenes, such as methylpyrimidine (**19**) and methylthiazole (**20**), were unsuccessful and led to inhibitory activities in the micromolar range (3.8–19.2 μM). The isopentyl-substituted analogs again demonstrated that the cyclopropylamide contributed significantly to the potency (**37**, 87 nM vs **36**, 138 nM). Furthermore, reducing the ring size of piperidine to four-membered azetidine also caused a 6-fold potency drop (**37** vs **38**). Finally, the phenoxy moiety was found to be a suitable replacement of 4-hydroxypiperidine and improved the inhibition dramatically (**12** and **13**, 57–89 nM). In comparison to the lead analogs (such as **5**, **6**, **36**, and **37**) with aqueous solubility greater than 62 μg/mL, the phenoxy analogs exhibited poor solubility (<1 and 6.1 μg/mL) for analogs **12** and **13**, respectively. As such, despite the potent inhibitory

Table 1. SAR of R² Portion of Theophylline-Based ALDH1A1 Inhibitors

hits 5–6 and analogs
11–14, 19–20, 26–38

Cpd	R ¹	R ²	hALDH1A1 IC ₅₀ ± SD (nM) ^a	RLM ^b (t _{1/2} , min)
5			40 ± 5 ^c	5
6			77 ± 15 ^c	23
11			570 ± 156	2
12			57 ± 9	8
13			89 ± 34	> 30
14			13.7 ± 4.9 (μM)	21
19			19.2 ± 3.3 (μM)	1
20			3.8 ± 1.1 (μM)	2
26			562 ± 98	2
27			213 ± 48	2
28			441 ± 212	3
29			245 ± 63	6
30			225 ± 51	4
31			840 ± 371	4
32			4.7 ± 2.2 (μM)	3
33			104 ± 21	5
34			84 ± 14	4
35			284 ± 59	2
36			138 ± 18	11
37			87 ± 71	17
38			537 ± 62	> 30

^aValues with standard deviation (SD) represent the average of three to six runs from one to two experiments. The IC₅₀ values are shown in nM unless otherwise specified. ^bRLM represents rat liver microsomal stability conducted at NCATS in the presence of NADPH. ^cIC₅₀ value was given based on resynthesized material.

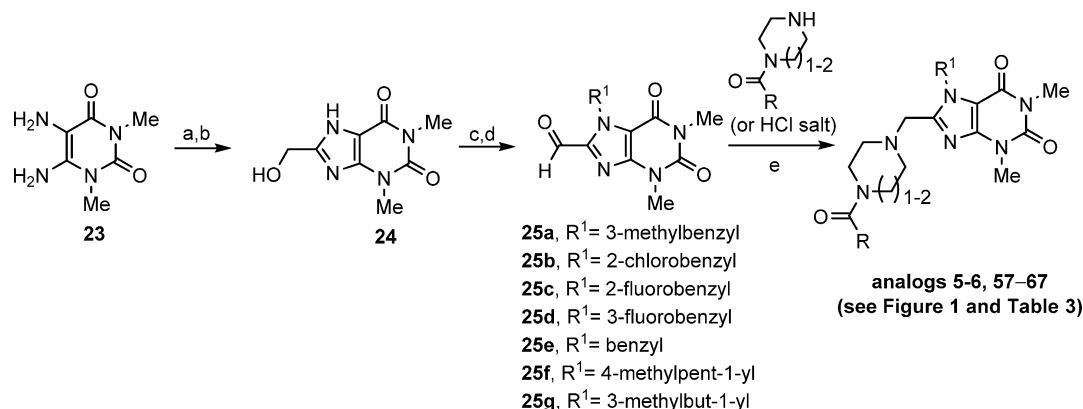
Table 2. SAR of R¹ Portion of Theophylline-Based ALDH1A1 Inhibitors

analogues 21–22, 39–56

Cpd	R ¹	hALDH1A1 IC ₅₀ ± SD (nM) ^a	RLM ^b (t _{1/2} , min)
21		214 ± 28	> 30
22	H	25.1 ± 5.9 (μM)	> 30
39		629 ± 179	14
40		1.8 ± 1.5 (μM)	8
41		1.5 ± 0.5 (μM)	> 30
42		545 ± 174	> 30
43		177 ± 49	21
44		876 ± 250	21
45		285 ± 101	20
46		153 ± 49	24
47		131 ± 60	4
48		12.5 ± 6.4 (μM)	> 30
49		91 ± 33	2
50		3.9 ± 1.3 (μM)	> 30
51		81 ± 11	3
52		76 ± 11	17
53		555 ± 173	25
54		30 ± 12	1
55		3.9 ± 0.7 (μM)	1
56		> 57 (μM)	> 30

^aValues with standard deviation (SD) represent the average of three to six runs from one to two experiments. The IC₅₀ values are shown in nM unless otherwise specified. ^bRLM represents rat liver microsomal stability conducted at NCATS in the presence of NADPH.

potency, these compounds were deprioritized for further development. Beyond the demonstrated potency increase by cyclopropylamide modification, no further improvement in RLM stability was observed. Other key SAR findings taken from Table 1 include the following: (1) the 3-methylbenzyl

Scheme 2. Synthesis of Piperazine-Substituted, Theophylline-Based ALDH1A1 Inhibitors^a

^aReagents and conditions: (a) 2-hydroxyacetic acid, neat, 100 °C, 3 h, 49%; (b) NaOH(aq), 100 °C, 2 h, **24** (82%); (c) R¹-Br, K₂CO₃, DMF, rt to 60 °C, 3-24 h; (d) Dess-Martin periodinane, CH₂Cl₂, 0 °C to rt, 1-2 h; (e) piperazine or homopiperazine derivatives (or its HCl salt), NaBH(OAc)₃, Et₃N, rt, 4 h.

Table 3. Combination of Favored R¹ Substitution and Piperazine-Type R² Substitution

Cpd	R ¹	R ²	hALDH1A1 IC ₅₀ ± SD (nM) ^a	RLM ^b (t _{1/2} , min)
57			33 ± 5	6
58			65 ± 14	26
59			256 ± 48	> 30
60			390 ± 73	20
61			69 ± 8	13
62			86 ± 26	20
63			35 ± 10	5
64 (NCT-501)			40 ± 23	> 30
65			92 ± 35	> 30
66			69 ± 31	> 30
67			320 ± 111	5

^aValues with standard deviation (SD) represent the average of three to six runs from one to two experiments. The IC₅₀ values are shown in nM unless otherwise specified. ^bRLM represents rat liver microsomal stability conducted at NCATS in the presence of NADPH.

group seemed responsible for RLM instability as suspected (e.g., **5** vs **6**; **12** vs **13**; **34** vs **37**), and (2) the methyl piperazine analogs are slightly more potent than 4-hydroxypiperidine analogs, e.g., **5** (40 nM) and **6** (77 nM) vs **27** (213 nM) and **36** (138 nM), respectively.

Given that the cyclopropylamide moiety improved inhibition of ALDH1A1, we maintained this motif on the second set of analogs aimed at addressing the relationships between R¹ substitution and RLM instability from newly identified leads **34** and **37**. Analogs with various substituted aryl and alkyl R¹ substitutions were synthesized and screened (Table 2). Removal of R¹ group (**22**) led to a significant loss in activity, while benzyl (**21**) or phenylethyl (**39**) only slightly diminished potency in a comparison with **34**. Importantly, these analogs exhibit improved RLM stability, leading us to suspect the 3-Me group as key factor in the observed RLM instability. This was further supported by the finding that the RLM stability is greatly influenced by substitution pattern of phenyl ring. For instance, electron-withdrawing groups, such as CF₃ (**41**), Cl (**42**), or F (**45**), are preferred, giving marked improvement in RLM stability (t_{1/2} ≥ 20 min), though the IC₅₀ values are decreased compared to the Me substitution (**34**). The electron-donating group, exemplified by OMe (**40**), is undesirable in both potency and RLM stability. Interestingly, moving these substitutions to 2-position, such as **43** and **46** vs **42** and **45**, respectively, gained potency back while improving RLM stability. However, the 2-F substitution did not overcome the undesired RLM issue caused by 3-Me substitution, as analog **47** had a RLM stability of only 4 min. Replacing the phenyl ring with pyridine produced analogs with improved RLM stability but with significantly lower potency (**48**, 12.5 μM). Finally, the bicyclic naphthylene substituent also produced potent analog **49** (91 nM) but again resulted in a RLM stability issue.

In parallel, investigation of alkyl type R¹ substitution was conducted (Table 2). Compared to lead compound **37**, the shorter alkyl chain (**50**) increased RLM stability, albeit with significant loss of potency to 3.9 μM, while the opposite results were obtained with longer alkyl chain analog **51** (81 nM; RLM, 3 min), leading us to focus on modifying the isopentyl portion. Changing to a more hydrophobic dimethylbutyl side chain (**52**) showed comparable potency (76 nM) and RLM stability (12 min) to **37**. Further tethering the dimethyl groups of the isopentyl moiety led to analogs with either improved RLM stability (example, **53**, RLM, 25 min) or retained potency (**54**, 30 nM) but not both. Surprisingly, the oxetane analog (**56**) completely lost inhibitory activity. The data obtained for R¹ modification suggest that hydrophobic interactions with enzyme in this region are preferred. This is consistent with

Table 4. Selectivity against Other ALDH Isozymes and Dehydrogenases^a

compd	IC ₅₀ (μM)					
	hALDH1A1	hALDH1B1	hALDH3A1	hALDH2	HPGD	HSD17β4
5	0.040	>57	24.3	2.4	>57	>57
6	0.077	>57	>57	>57	>57	>57
12	0.057	>57	24.3	6.1	>57	>57
13	0.089	>57	1.5	2.4	>57	>57
27	0.213	>57	4.9	3.9	>57	>57
34	0.084	>57	>57	15.3	>57	>57
36	0.138	>57	>57	>57	>57	>57
37	0.087	>57	>57	2.4	>57	>57
57	0.033	>57	>57	7.7	>57	>57
58	0.065	>57	>57	>57	>57	>57
64	0.040	>57	>57	>57	>57	>57

^aCompounds noted as >57 μM represent a very weak or no inhibition [efficacy of ≤50% of full inhibition at highest tested concentration (57 μM)].

reported cocrystallized structure of a theophylline-based analog that R¹ substitution points toward the space surrounded by greasy residues Phe171 and Phe466.²⁷

Piperazine containing analogs generally gave better potency (e.g., 5 and 6 vs 27 and 36, respectively), so we decided to pursue another set of compounds containing this moiety while varying the R¹ substitutions as shown in Table 3. A direct comparison of piperazine containing analogs 57, 58, 61, 62, 63, and 64 vs 4-hydropiperidine analogs 34, 21, 43, 45, 51, and 37, respectively, confirmed our expectation to further improve potency. 2-Fluorobenzyl substitution was the exception and resulted in a 2-fold loss of potency (60, 390 nM vs 46, 153 nM). As seen with analogs 34 and 51, the 3-methylbenzyl (57) and isohexyl (63) substitutions exhibited excellent inhibition but suffered low RLM stability. Ring expansion of piperazine to homopiperazine (64 vs 67) not only caused an 8-fold loss of potency but also decreased RLM stability significantly. These data, together with the result from ring constrained analog 38, indicate that six-membered rings, such as piperazine or piperidine, are preferred. Overall, the isopentyl R¹ substitution and piperazine amide type of R² substitution appear to be the optimized combination in terms of potency and eADME (e.g., RLM stability), exemplified as compound 64 (NCT-501) that is suitable for further evaluation.

Selectivity Evaluation. With all analogs examined against ALDH1A1, a set of potent analogs with representative R¹ substitutions (3-methylbenzyl and isopentyl) and variations in R² substitutions were selected and screened against ALDH isozymes (examples ALDH1B1, ALDH3A1, and ALDH2) and other dehydrogenases such as 15-hydroxyprostaglandin dehydrogenase (HPGD) and type 4 hydroxysteroid dehydrogenase (HSD17β4).³⁰ In general, ALDH1A1 shares nearly 70% sequence identity to mitochondrial ALDH2 and ALDH1B1 isozymes, less than 50% sequence identity to ALDH3A1, and significant less similarity to HPGD or HSD17β4. As the results compiled in Table 4, these theophylline-based analogs exhibited no inhibition toward ALDH1B1, HPGD, or HSD17β4. Some low inhibitory activities in the micromolar range against ALDH3A1 and/or ALDH2 were observed and were seemingly dependent on the R¹ or R² substitution pattern. For instance, the alkyl type isopentyl R¹ substitution, such as analogs 6, 36, and 64, typically showed better selectivity over other ALDH isozymes and other dehydrogenases, while the 3-methylbenzyl exhibited some degree of inhibition toward ALDH3A1 and ALDH2 (examples 5, 27, and 57). In contrast, the phenoxy type R² substitution seemed to play a vital role in picking up

ALDH3A1 and ALDH2 inhibitions (12 and 13). Finally, removal of 3-methyl group resulted in enhanced selectivity (e.g., 58 vs 57). These data, along with the above-mentioned SAR and structure–property relationship (SPR) explorations, suggested that compound 64 should be selected for further evaluation and characterization. Accordingly, compound 64 was profiled for off-target kinase activity using DiscoverX KINOMEScan screening platform. The results indicated 64 is a clean inhibitor with no significant hits (i.e., inhibition of ≥55% at 10 μM) observed against more than 450 human kinases (Supporting Information Figure S1). To further evaluate any potential off-target activity of 64, we profiled it against the gpcrMAX panel which contains 168 GPCRs covering 60 receptor families and is run in both agonist and antagonist mode. As with the kinase profile, compound 64 demonstrated very little activity in either agonist or antagonist mode (Supporting Information Figure S2).

Mechanism Studies. During the preparation of this manuscript, Hurley and co-workers published an X-ray crystal structure of a similar theophylline-based analog with ALDH1A1.²⁷ This structure along with kinetic studies indicated that these analogs are substrate noncompetitive inhibitors, which bind near the solvent exposed exit of substrate-binding site. Independent kinetic studies in our laboratory corroborated these findings (data not shown). This mode differs from the previously reported indolinedione and tricyclic pyrimidinone type of inhibitors (e.g., 3 and 4) which both demonstrated substrate competitive inhibition.^{21,22} To further investigate the mechanism of action, a rapid dilution experiment using 64 was conducted to determine the reversibility of the inhibition. The reaction time courses were collected after incubation with 64 at an IC₉₀ concentration (red triangle, Figure 2) and rapid dilution of enzymatic reaction. The diluted sample rapidly recovered enzymatic activity (orange box), similar to the low-compound incubated control (blue triangle) or in the absence (green circle) of inhibitor, indicating that compound 64 demonstrates reversible inhibition of ALDH1A1.

Pharmacokinetics and in Vitro ADME Profiles. After demonstrating desirable potency and selectivity with a better understanding of the mechanism of action, compound 64, which possessed favorable kinetic aqueous solubility (>60 μg/mL) and RLM stability (>30 min), was further evaluated for its pharmacokinetics (PK) in CD1 mice. The compound was dosed at 2 mg/kg, 10 mg/kg, and 30 mg/kg for intravenous (iv), oral (po), and intraperitoneal (ip) administration, respectively. Brain and liver tissues are also collected and

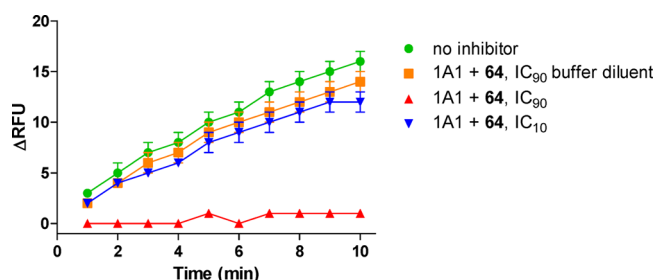


Figure 2. Rapid dilution assay. The experiment was conducted using **64** as the inhibitor in the presence of ALDH1A1 (20 nM), substrate (propionaldehyde, 80 μ M), and cofactor (NAD^+ , 1 mM) in 1536-well format.

analyzed after po administration to further evaluate the feasibility of potential long-term treatment for metabolic indications. The PK result compiled in Table 5 revealed that analog **64** has more desirable plasma exposure for IP ($\text{AUC}_{24\text{h}} = 5670 \text{ h}\cdot\text{ng}/\text{mL}$; 30 mg/kg) than po ($\text{AUC}_{24\text{h}} = 484 \text{ h}\cdot\text{ng}/\text{mL}$; 10 mg/kg) along with 100% and 29% bioavailability, respectively. (see Supporting Information Table S1 and Figures S4 and S5 for more details). Reasonable volume of distribution ($V_{\text{ss}} = 1.8 \text{ L}/\text{kg}$) but short half-life ($t_{1/2} < 1 \text{ h}$) and high clearance level ($\text{CL} = 98 \text{ mL min}^{-1} \text{ kg}^{-1}$) indicate that **64** is well absorbed and distributed but rapidly metabolized and/or excreted. This is consistent with the finding of short $t_{1/2}$ of CD1 mouse liver microsomal stability (17 min, multipoint format).³¹ Carefully analyzing the in vitro metabolism of **64** (see Supporting Information) and the plasma sample from PK studies by ultraperformance LC MS/MS suggested the hydroxylation at the terminal of isopentyl side chain and the hydrolysis of cyclopropylamide moiety are the major metabolites. In addition, the high clearance presumably also attributed partially from its low plasma protein binding (68.6% bound) which increases the fraction of unbound drug making it more susceptible to being metabolized and/or excreted. Tissue analysis revealed that **64** is distributed at a higher drug concentration in liver ($L/P = 3.88$) where the ALDH activity expresses the highest level.³² This finding also supported that the phase I modification in liver seems to be the major issue for elimination, since **64** possessed reasonable in vitro stability in CD1 mouse plasma ($>60 \text{ min}$). Notably, despite the low drug exposure in brain, brain/plasma ratio ($B/P = 0.54$) suggests that **64** does not penetrate the blood–brain barrier. As such, potential CNS related effects would need to be considered particularly for a long-term treatment. Finally, the permeability measured in Caco-2 cell line (efflux ratio of $P_{\text{app}}(\text{B}\rightarrow\text{A})$ ($10^{-6} \text{ cm}/\text{s}$)/ $P_{\text{app}}(\text{A}\rightarrow\text{B})$ ($10^{-6} \text{ cm}/\text{s}$) = 19.58/19.28 = 1.02) also indicates that **64** exhibits excellent permeability and does not seem to be a substrate of transporters, such as P-gp. Given the favorable solubility and Caco-2 permeability data for this chemotype, the

low oral bioavailability seems to be attributed to the rapid clearance via first pass metabolism as mentioned above.

CONCLUSION

The overexpression of specific ALDH isozymes in certain CSCs suggests ALDHs as potential targets for cancer and CSC-directed therapeutics. In addition, it has been shown that selective targeting of ALDH isozymes prevents spheroid formation in vitro and the size of xenograft tumors formed in vivo.³³ In this study, we performed a systematic medicinal chemistry optimization of theophylline-based qHTS hits that ultimately led to potent ALDH1A1 inhibitors with improved eADME properties. This chemotype demonstrated a high degree of selectivity over other ALDH isozymes (ALDH1B1, ALDH3A1, and ALDH2) and other dehydrogenases (HPGD and HSD17 β 4). A rapid dilution experiment suggested the selected analog **64** is a reversible inhibitor. The PK study demonstrated that analog **64** had reasonable drug exposure via ip administration and should be suitable for in vivo proof of concept animal studies. However, further improvement of the half-life and oral bioavailability would be beneficial if this compound is to be dosed po. Current studies are focused on evaluating this class of molecules in cell-based studies (e.g., patient-derived CSCs) and other disease-relevant models, which could benefit from selective pharmacological ALDH1A1 inhibition. As the combined activity of two or more ALDH isoforms is likely to be associated with a specific cancer, the feasibility of using a combination of isoform selective inhibitors or a dual inhibitor as a clinical prognostic application should also be considered.¹⁵

EXPERIMENTAL SECTION

General Methods for Chemistry. All air or moisture sensitive reactions were performed under positive pressure of nitrogen with oven-dried glassware. Chemical reagents and anhydrous solvents were obtained from commercial sources and used as is. Preparative purification was performed on a Waters semipreparative HPLC instrument. The column used was a Phenomenex Luna C18 (5 μm , 30 mm \times 75 mm) at a flow rate of 45 mL/min. The mobile phase consisted of acetonitrile and water (each containing 0.1% trifluoroacetic acid). A gradient from 10% to 50% acetonitrile over 8 min was used during the purification. Fraction collection was triggered by UV detection (220 nm). Analytical analysis for purity was determined by two different methods denoted as final QC methods 1 and 2.

Method 1. Analysis was performed on an Agilent 1290 Infinity series HPLC instrument. UHPLC long gradient equivalent from 4% to 100% acetonitrile (0.05% trifluoroacetic acid) in water over 3 min run time of 4.5 min with a flow rate of 0.8 mL/min. A Phenomenex Luna C18 column (3 μm , 3 mm \times 75 mm) was used at a temperature of 50 $^{\circ}\text{C}$.

Method 2. Analysis was performed on an Agilent 1260 with a 7 min gradient from 4% to 100% acetonitrile (containing 0.025% trifluoroacetic acid) in water (containing 0.05% trifluoroacetic acid) over 8 min run time at a flow rate of 1 mL/min. A Phenomenex Luna C18 column

Table 5. Pharmacokinetic Results of **64** in CD1 Mice

admin (dosage)	sample	C_{max} (ng/mL)	$T_{1/2}$ (h)	$\text{AUC}_{24\text{h}}$ (h \cdot ng/mL)	V_{ss} (L/kg)	CL ($\text{mL min}^{-1} \text{ kg}^{-1}$)	F (%)
iv (2 mg/kg) ^a	plasma	2070 ^b	0.5	332	1.8	98	
ip (30 mg/kg) ^a	plasma	8080	0.7	5670			100
po (10 mg/kg) ^a	plasma	696	0.4	484			29
po (10 mg/kg) ^a	brain	1130	0.4	261 ^c			
po (10 mg/kg) ^a	liver	2690	0.4	1880 ^d			

^a $n = 3$. The compound (**64**) was formulated as solution in 30% HP β CD in saline. ^b $C_{\text{max}} = C_0$ ($t = 0$) for iv administration. ^cBrain/plasma (B/P) ratio of 0.54. ^dLiver/plasma (L/P) ratio of 3.88.

(3 μ m, 3 mm \times 75 mm) was used at a temperature of 50 °C. Purity determination was performed using an Agilent diode array detector for both method 1 and method 2. Mass determination was performed using an Agilent 6130 mass spectrometer with electrospray ionization in the positive mode. All of the analogs for assay have purity greater than 95% based on both analytical methods. ^1H NMR spectra were recorded on Varian 400 MHz spectrometers. High resolution mass spectrometry results were recorded on Agilent 6210 time-of-flight LC/MS system.

Representative Synthetic Procedures. Preparation of 8-Chloro-1,3-dimethyl-7-(3-methylbenzyl)-1H-purine-2,6-(3H,7H)-dione (8). To a mixture of 8-chloro-1,3-dimethyl-1H-purine-2,6-(3H,7H)-dione (7, 2.15 g, 10 mmol) and K_2CO_3 (2.07 g, 15 mmol) was added *N,N*-dimethylformamide (12 mL). The mixture was stirred at rt for 5 min, and 1-(bromomethyl)-3-methylbenzene (2.22 g, 12 mmol) was added. The mixture was stirred at rt for 30 min and then heated at 60 °C for 2 h. The mixture was then dropped into vigorously stirred H_2O (250 mL). The resulting solid was filtered, washed with H_2O (30 mL \times 2), hexane (5 mL \times 2), and then dried to give 8-chloro-1,3-dimethyl-7-(3-methylbenzyl)-1H-purine-2,6-(3H,7H)-dione (8, 3.12 g, 9.79 mmol, 98% yield). ^1H NMR (400 MHz, chloroform-*d*) δ 7.23 (dd, J = 8.2, 7.4 Hz, 1H), 7.17–7.09 (m, 3H), 5.51 (s, 2H), 3.55 (s, 3H), 3.40 (s, 3H), 2.33 (s, 3H). LC–MS (method 1): t_{R} = 3.40 min, m/z ($\text{M} + \text{H}$) $^+$ = 319.

Preparation of Ethyl 4-(1,3-Dimethyl-7-(3-methylbenzyl)-2,6-dioxo-2,3,6,7-tetrahydro-1H-purin-8-yl)piperazine-1-carboxylate, TFA (11). In a microwave tube was placed 8-chloro-1,3-dimethyl-7-(3-methylbenzyl)-1H-purine-2,6-(3H,7H)-dione (8, 159 mg, 0.5 mmol) and ethyl piperazine-1-carboxylate (237 mg, 1.5 mmol), and to the mixture was added DMSO (1 mL). The mixture was sealed and heated at 160 °C under microwave irradiation for 30 min. The crude mixture was filtered through a filter and submitted for purification by semipreparative HPLC to give ethyl 4-(1,3-dimethyl-7-(3-methylbenzyl)-2,6-dioxo-2,3,6,7-tetrahydro-1H-purin-8-yl)piperazine-1-carboxylate, TFA (11, 160 mg, 0.289 mmol, 58% yield). ^1H NMR (400 MHz, DMSO-*d*₆) δ 7.19 (t, J = 7.6 Hz, 1H), 7.11–6.98 (m, 2H), 6.93 (d, J = 7.6 Hz, 1H), 5.34 (s, 2H), 4.02 (q, J = 7.1 Hz, 2H), 3.39 (m, 7H), 3.17 (s, 3H), 3.13–3.01 (m, 4H), 2.24 (s, 3H), 1.16 (t, J = 7.1 Hz, 3H). LC–MS (method 2): t_{R} = 5.44 min, m/z ($\text{M} + \text{H}$) $^+$ = 441. HRMS calculated for $\text{C}_{22}\text{H}_{29}\text{N}_6\text{O}_4$ ($\text{M} + \text{H}$) $^+$: 441.2245. Found: 441.2262.

Preparation of 4-((1,3-Dimethyl-7-(3-methylbenzyl)-2,6-dioxo-2,3,6,7-tetrahydro-1H-purin-8-yl)oxy)-*N*-methylbenzamide, TFA (12). *Step 1.* In a microwave tube was placed 8-chloro-1,3-dimethyl-7-(3-methylbenzyl)-1H-purine-2,6-(3H,7H)-dione (8, 319 mg, 1 mmol), methyl 4-hydroxybenzoate (183 mg, 1.2 mmol), and K_2CO_3 (207 mg, 1.5 mmol). Then, DMF (3 mL) was added. The mixture was sealed and heated at 160 °C under microwave irradiation for 1 h. The mixture was poured into stirred H_2O (60 mL), and the solid was filtered. The solid was then dissolved in CH_2Cl_2 and was purified by silica gel chromatography using 50–100% EtOAc/hexane as the eluent to give methyl 4-((1,3-dimethyl-7-(3-methylbenzyl)-2,6-dioxo-2,3,6,7-tetrahydro-1H-purin-8-yl)oxy)benzoate (361 mg, 0.83 mmol, 83% yield). ^1H NMR (400 MHz, chloroform-*d*) δ 8.14–8.03 (m, 2H), 7.35–7.28 (m, 2H), 7.23–7.20 (m, 3H), 7.13–7.07 (m, 1H), 5.43 (s, 2H), 3.93 (s, 3H), 3.45 (s, 3H), 3.42 (s, 3H), 2.30 (d, J = 0.8 Hz, 3H). LC–MS (method 2): t_{R} = 6.03 min, m/z ($\text{M} + \text{H}$) $^+$ = 435.

Step 2. To a solution of methyl 4-((1,3-dimethyl-7-(3-methylbenzyl)-2,6-dioxo-2,3,6,7-tetrahydro-1H-purin-8-yl)oxy)benzoate (148 mg, 0.34 mmol) in THF/MeOH (4 mL/0.5 mL) was added $\text{LiOH}_{(\text{aq})}$ (1.5 N, 2 mL). The mixture was stirred at 50 °C for 3 h, and $\text{HCl}_{(\text{aq})}$ (1 N, 4 mL) was added. Then hexane (10 mL) was added and the resulting solid was filtered, washed with H_2O (2 mL \times 2), 5% Et₂O/hexane (2 mL \times 2), and then dried to give 4-((1,3-dimethyl-7-(3-methylbenzyl)-2,6-dioxo-2,3,6,7-tetrahydro-1H-purin-8-yl)oxy)benzoic acid (69 mg, 0.164 mmol, 48% yield). ^1H NMR (400 MHz, DMSO-*d*₆) δ 13.03 (s, 1H), 8.04–7.94 (m, 2H), 7.44–7.34 (m, 2H), 7.22 (t, J = 7.6 Hz, 1H), 7.15–7.03 (m, 3H), 5.39 (s, 2H), 3.29 (s, 3H), 3.22 (s, 3H), 2.24 (s, 3H). LC–MS (method 2): t_{R} = 5.08 min, m/z ($\text{M} + \text{H}$) $^+$ = 421.

Step 3. To a mixture of 4-((1,3-dimethyl-7-(3-methylbenzyl)-2,6-dioxo-2,3,6,7-tetrahydro-1H-purin-8-yl)oxy)benzoic acid (42 mg, 0.1 mmol) and HATU (95 mg, 0.25 mmol) were added DMF (1 mL), methanamine (2 M in THF, 1 mL, 2 mmol), and then Hunig's base (0.087 mL, 0.5 mmol). The mixture was stirred at rt for 2 h. The mixture was filtered through a filter and submitted for purification by semipreparative HPLC to give 4-((1,3-dimethyl-7-(3-methylbenzyl)-2,6-dioxo-2,3,6,7-tetrahydro-1H-purin-8-yl)oxy)-*N*-methylbenzamide, TFA (12, 25 mg, 0.046 mmol, 46% yield). ^1H NMR (400 MHz, DMSO-*d*₆) δ 8.45 (q, J = 4.5 Hz, 1H), 7.93–7.82 (m, 2H), 7.40–7.33 (m, 2H), 7.22 (t, J = 7.5 Hz, 1H), 7.18–7.04 (m, 3H), 5.39 (s, 2H), 3.28 (s, 3H), 3.22 (s, 3H), 2.77 (d, J = 4.5 Hz, 3H), 2.24 (s, 3H). LC–MS (method 2): t_{R} = 4.87 min, m/z ($\text{M} + \text{H}$) $^+$ = 434. HRMS calculated for $\text{C}_{23}\text{H}_{24}\text{N}_5\text{O}_4$ ($\text{M} + \text{H}$) $^+$: 434.1823. Found: 434.1834.

Preparation of 1,3-Dimethyl-7-(3-methylbenzyl)-8-(piperidin-4-yloxy)-1H-purine-2,6-(3H,7H)-dione, HCl (14). *Step 1.* To a solution of *tert*-butyl 4-hydroxypiperidine-1-carboxylate (403 mg, 2 mmol) in DMF (4 mL) under N_2 at rt was added NaH (72 mg, 3 mmol). After 5 min stirring, 8-chloro-1,3-dimethyl-7-(3-methylbenzyl)-1H-purine-2,6-(3H,7H)-dione (8, 638 mg, 2 mmol) was added. The mixture was then stirred at rt for 30 min and was poured into EtOAc/ H_2O (10 mL/10 mL). The aqueous layer was extracted with EtOAc (5 mL \times 2). The combined organic layer was dried (Na_2SO_4) and filtered. After removal of solvent, the crude product was purified by silica gel chromatography using 20–60–80% EtOAc/hexane as the eluent to give *tert*-butyl 4-((1,3-dimethyl-7-(3-methylbenzyl)-2,6-dioxo-2,3,6,7-tetrahydro-1H-purin-8-yl)oxy)piperidine-1-carboxylate (857 mg, 1.77 mmol, 89% yield). ^1H NMR (400 MHz, chloroform-*d*) δ 7.23–7.11 (m, 3H), 7.08 (ddq, J = 7.3, 1.6, 0.8 Hz, 1H), 5.25 (s, 2H), 5.17 (dt, J = 7.4, 3.7 Hz, 1H), 3.57 (ddd, J = 13.6, 7.6, 3.9 Hz, 2H), 3.49 (s, 3H), 3.40 (s, 3H), 3.39–3.30 (m, 2H), 2.31 (d, J = 0.8 Hz, 3H), 1.97 (m, 2H), 1.79 (m, 2H), 1.47 (s, 9H).

Step 2. To a solution of *tert*-butyl 4-((1,3-dimethyl-7-(3-methylbenzyl)-2,6-dioxo-2,3,6,7-tetrahydro-1H-purin-8-yl)oxy)piperidine-1-carboxylate (945 mg, 1.95 mmol) in 1,4-dioxane (2 mL) was added HCl (4 M in 1,4-dioxane, 4 mL). The mixture was stirred at rt for overnight, and the mixture was concentrated to remove all the solvent. Then the product was dried in vacuo to give 1,3-dimethyl-7-(3-methylbenzyl)-8-(piperidin-4-yloxy)-1H-purine-2,6-(3H,7H)-dione, HCl (14, 796 mg, 1.90 mmol, 97% yield). The material was used without further purification. Some material was submitted for purification by semipreparative HPLC to give TFA salt of 14 for screening. ^1H NMR (TFA salt, 400 MHz, DMSO-*d*₆) δ 8.50 (s, 2H), 7.27–7.14 (m, 1H), 7.13–7.00 (m, 3H), 5.30–5.13 (m, 3H), 3.36 (s, 3H), 3.20 (s, 3H), 3.17–3.04 (m, 4H), 2.26 (s, 3H), 2.12 (m, 2H), 1.92 (m, 2H). LC–MS (method 1): t_{R} = 2.70 min, m/z ($\text{M} + \text{H}$) $^+$ = 384.

Preparation of 1,3-Dimethyl-7-(3-methylbenzyl)-8-((1-(4-methylpyrimidin-2-yl)piperidin-4-yl)oxy)-1H-purine-2,6-(3H,7H)-dione, TFA (19). In a microwave tube was placed 1,3-dimethyl-7-(3-methylbenzyl)-8-(piperidin-4-yloxy)-1H-purine-2,6-(3H,7H)-dione, HCl (14, 63 mg, 0.15 mmol), 2-chloro-4-methylpyrimidine (38.6 mg, 0.3 mmol), and K_2CO_3 (83 mg, 0.6 mmol). Then, DMF (1 mL) was added sequentially. The mixture was sealed and heated at 160 °C under microwave irradiation for 1 h. The mixture was filtered and submitted for purification by semipreparative HPLC to give 1,3-dimethyl-7-(3-methylbenzyl)-8-((1-(4-methylpyrimidin-2-yl)piperidin-4-yl)oxy)-1H-purine-2,6-(3H,7H)-dione, TFA (19, 41.3 mg, 0.07 mmol, 47% yield). ^1H NMR (400 MHz, DMSO-*d*₆) δ 8.20 (d, J = 5.0 Hz, 1H), 7.18 (t, J = 7.6 Hz, 1H), 7.11 (t, J = 1.7 Hz, 1H), 7.05 (dt, J = 7.0, 1.4 Hz, 2H), 6.52 (dd, J = 5.0, 1.3 Hz, 1H), 5.26–5.22 (m, 1H), 5.21 (s, 2H), 3.77 (m, 4H), 3.37 (s, 3H), 3.20 (s, 3H), 2.27 (s, 3H), 2.19 (s, 3H), 2.02–1.87 (m, 2H), 1.77–1.62 (m, 2H). LC–MS (method 2): t_{R} = 5.15 min, m/z ($\text{M} + \text{H}$) $^+$ = 476. HRMS calculated for $\text{C}_{25}\text{H}_{30}\text{N}_7\text{O}_3$ ($\text{M} + \text{H}$) $^+$: 476.2405. Found: 476.2424.

Preparation of 7-Benzyl-8-((1-(cyclopropanecarbonyl)piperidin-4-yl)oxy)-1,3-dimethyl-1H-purine-2,6-(3H,7H)-dione (21). To a solution of 7-benzyl-1,3-dimethyl-8-(piperidin-4-yloxy)-1H-purine-2,6-(3H,7H)-dione, HCl (16, 0.61 g, 1.5 mmol) in CH_2Cl_2 (5 mL) was added Et_3N (1.25 mL, 9 mmol) and then cyclo-

propanecarbonyl chloride (0.31 g, 3 mmol) dropwise. The mixture was stirred at rt for 30 min and then poured into EtOAc/H₂O/Na₂CO_{3(aq)} (50 mL/25 mL/25 mL). The organic layer was washed with H₂O (50 mL), dried (Na₂SO₄), and filtered. After removal of solvent, the product was dried to give 7-benzyl-8-((1-(cyclopropanecarbonyl)piperidin-4-yl)oxy)-1,3-dimethyl-1H-purine-2,6(3H,7H)-dione (**21**, 630 mg, 96%). This material was used for the next step without further purification. Small amount of product was submitted for purification by semipreparative HPLC to give TFA salt of **21** for screening. ¹H NMR (TFA salt, 400 MHz, DMSO-*d*₆) δ 7.46–7.11 (m, 5H), 5.26 (s, 2H), 5.20 (dt, *J* = 7.0, 3.4 Hz, 1H), 3.67 (s, 2H), 3.48 (s, 2H), 3.36 (s, 3H), 3.20 (s, 3H), 1.96 (m, 3H), 1.68 (m, 2H), 0.76–0.60 (m, 4H). LC–MS (method 1): *t*_R = 3.24 min, *m/z* (M + H)⁺ = 438. HRMS calculated for C₂₃H₂₇N₅O₄Na (M + Na)⁺: 460.1955. Found: 460.1977.

Preparation of 8-((1-(Cyclopropanecarbonyl)piperidin-4-yl)oxy)-1,3-dimethyl-1H-purine-2,6(3H,7H)-dione (22**).** In a two-neck flask was placed 7-benzyl-8-((1-(cyclopropanecarbonyl)piperidin-4-yl)oxy)-1,3-dimethyl-1H-purine-2,6(3H,7H)-dione (**21**, 1.75 g, 4 mmol) and Pd(OH)₂ (0.56 g, 0.8 mmol). Then, EtOH/EtOAc (40 mL/20 mL) was added. The air was removed and refilled with H₂ (3 times). The mixture was heated to 70 °C for 24 h under H₂ balloon. After cooling to rt, the mixture was filtered through Celite and eluted with CH₂Cl₂. The filtrate was concentrated and the solid was triturated with 2% EtOAc/hexane and then dried in vacuo to give 8-((1-(cyclopropanecarbonyl)piperidin-4-yl)oxy)-1,3-dimethyl-1H-purine-2,6(3H,7H)-dione (**22**, 1.04 g, 3 mmol, 75% yield). ¹H NMR (400 MHz, chloroform-*d*) δ 11.15 (s, 1H), 5.26 (dt, *J* = 7.2, 3.6 Hz, 1H), 3.90 (br s, 2H), 3.75–3.57 (m, 2H), 3.55 (s, 3H), 3.43 (s, 3H), 2.08 (br s, 2H), 1.90 (br s, 2H), 1.81–1.73 (m, 1H), 1.00 (dt, *J* = 4.7, 3.1 Hz, 2H), 0.79 (dt, *J* = 8.0, 3.3 Hz, 2H). LC–MS (method 2): *t*_R = 3.51 min, *m/z* (M + H)⁺ = 348. HRMS calculated for C₁₆H₂₂N₅O₄ (M + H)⁺: 348.1666. Found: 348.1677.

Preparation of 7-Isopentyl-1,3-dimethyl-2,6-dioxo-2,3,6,7-tetrahydro-1H-purine-8-carbaldehyde (25g**).** *Step 1.* To a mixture of 8-(hydroxymethyl)-1,3-dimethyl-1H-purine-2,6(3H,7H)-dione (**24**, 1.05 g, 5 mmol) and K₂CO₃ (2.073 g, 15 mmol) was added *N,N*-dimethylformamide (15 mL). The mixture was stirred at rt for 5 min, and 1-bromo-3-methylbutane (2.398 mL, 20 mmol) was added. The mixture was heated at 60 °C for overnight and was poured into EtOAc/H₂O (80 mL/80 mL). The organic layer was washed with H₂O (80 mL), dried (Na₂SO₄), and then filtered. After removal of solvent, the product was purified by silica gel chromatography using 80–100% EtOAc/hexane as the eluent to give 8-(hydroxymethyl)-7-isopentyl-1,3-dimethyl-1H-purine-2,6(3H,7H)-dione (1.21 g, 4.32 mmol, 86% yield). ¹H NMR (400 MHz, chloroform-*d*) δ 4.75 (dd, *J* = 6.0, 0.9 Hz, 2H), 4.39–4.23 (m, 2H), 3.56 (d, *J* = 0.9 Hz, 3H), 3.41 (d, *J* = 0.8 Hz, 3H), 2.71 (td, *J* = 6.1, 3.1 Hz, 1H), 1.80–1.62 (m, 3H), 1.06–0.92 (m, 6H). LC–MS (method 1): *t*_R = 2.76 min, *m/z* (M + H)⁺ = 281.

Step 2. To a solution of 8-(hydroxymethyl)-7-isopentyl-1,3-dimethyl-1H-purine-2,6(3H,7H)-dione (1550 mg, 5.53 mmol) in DCM (15 mL) was added Dess–Martin periodinane (3283 mg, 7.74 mmol) at 0 °C. After 10 min, the mixture was stirred at rt for 2 h. The mixture was concentrated and the residue was purified by silica gel chromatography using 30–60% EtOAc/hexane as the eluent to give 7-isopentyl-1,3-dimethyl-2,6-dioxo-2,3,6,7-tetrahydro-1H-purine-8-carbaldehyde (**25g**, 1160 mg, 4.17 mmol, 75% yield). ¹H NMR (400 MHz, chloroform-*d*) δ 9.91 (s, 1H), 4.94–4.61 (m, 2H), 3.62 (s, 3H), 3.44 (s, 3H), 1.87–1.61 (m, 3H), 1.00 (d, *J* = 6.2 Hz, 6H). LC–MS (method 1): *t*_R = 3.30 min, *m/z* (M + H)⁺ = 279.

Preparation of 8-((1-(Cyclopropanecarbonyl)piperidin-4-yl)oxy)-1,3-dimethyl-7-(3-methylbenzyl)-1H-purine-2,6(3H,7H)-dione, TFA (34**).** To a solution of 1,3-dimethyl-7-(3-methylbenzyl)-8-(piperidin-4-yloxy)-1H-purine-2,6(3H,7H)-dione, HCl (**14**, 42 mg, 0.1 mmol) in CH₂Cl₂ (2 mL) were added Et₃N (0.07 mL, 0.5 mmol) and then cyclopropanecarbonyl chloride (21 mg, 0.2 mmol) dropwise. The mixture was stirred at rt for 30 min. MeOH (0.2 mL) was added and stirred for another 30 min. The mixture was concentrated, dissolved in DMSO (2 mL), filtered through a filter, and then submitted for

purification by semipreparative HPLC to give 8-((1-(cyclopropanecarbonyl)piperidin-4-yl)oxy)-1,3-dimethyl-7-(3-methylbenzyl)-1H-purine-2,6(3H,7H)-dione, TFA (**34**, 25.5 mg, 0.045 mmol, 45% yield). ¹H NMR (400 MHz, DMSO-*d*₆) δ 7.20 (t, *J* = 7.5 Hz, 1H), 7.14–7.03 (m, 3H), 5.22 (s, 2H), 5.19 (dd, *J* = 6.8, 3.4 Hz, 1H), 3.66–3.40 (m, 4H), 3.36 (s, 3H), 3.20 (s, 3H), 2.24 (s, 3H), 1.96 (m, 3H), 1.69 (m, 2H), 0.78–0.59 (m, 4H). LC–MS (method 2): *t*_R = 5.15 min, *m/z* (M + H)⁺ = 452. HRMS calculated for C₂₄H₂₉N₅O₄Na (M + Na)⁺: 474.2112. Found: 474.2123.

Preparation of 8-((1-(Cyclopropanecarbonyl)piperidin-4-yl)oxy)-1,3-dimethyl-7-phenethyl-1H-purine-2,6(3H,7H)-dione, TFA (39**).** To a mixture of 8-((1-(cyclopropanecarbonyl)piperidin-4-yl)oxy)-1,3-dimethyl-1H-purine-2,6(3H,7H)-dione (**22**, 20.8 mg, 0.06 mmol) and K₂CO₃ (16.6 mg, 0.12 mmol) was added *N,N*-dimethylformamide (1 mL). The mixture was stirred at rt for 5 min, and (2-bromoethyl)benzene (33.3 mg, 0.18 mmol) was added. The mixture was heated at 50 °C for 3 h. The mixture was filtered through a filter and submitted for purification by semipreparative HPLC to give 8-((1-(cyclopropanecarbonyl)piperidin-4-yl)oxy)-1,3-dimethyl-7-phenethyl-1H-purine-2,6(3H,7H)-dione, TFA (**39**, 8.9 mg, 0.016 mmol, 26% yield). ¹H NMR (400 MHz, DMSO-*d*₆) δ 7.27–7.13 (m, 3H), 7.09–7.03 (m, 2H), 4.96 (dt, *J* = 7.1, 3.5 Hz, 1H), 4.22 (t, *J* = 6.7 Hz, 2H), 3.43 (br s, 4H), 3.35 (s, 3H), 3.23 (s, 3H), 2.99 (t, *J* = 6.7 Hz, 2H), 1.95 (t, *J* = 7.3, 5.1 Hz, 1H), 1.78 (m, 2H), 1.45 (m, 2H), 0.70 (t, *J* = 6.4 Hz, 4H). LC–MS (method 2): *t*_R = 5.08 min, *m/z* (M + H)⁺ = 452. HRMS calculated for C₂₄H₃₀N₅O₄ (M + H)⁺: 452.2292. Found: 452.2275.

Preparation of 7-(2-Cyclohexylethyl)-8-((1-(Cyclopropanecarbonyl)piperidin-4-yl)oxy)-1,3-dimethyl-1H-purine-2,6(3H,7H)-dione, TFA (54**).** In a microwave tube were placed 8-((1-(cyclopropanecarbonyl)piperidin-4-yl)oxy)-1,3-dimethyl-1H-purine-2,6(3H,7H)-dione (**22**, 20.84 mg, 0.06 mmol) and 2-cyclohexylethanol (23.08 mg, 0.180 mmol). The tube was sealed, and the air was removed and then refilled with N₂. Then, (*E*)-di-*tert*-butyl diazene-1,2-dicarboxylate (41.4 mg, 0.180 mmol) and Ph₃P (47.2 mg, 0.180 mmol) in THF (1 mL) was added, and the mixture was stirred at rt for 3 h. The mixture was concentrated, redissolved in DMF, filtered through a filter, and then submitted for purification by semipreparative HPLC to give 7-(2-cyclohexylethyl)-8-((1-(cyclopropanecarbonyl)piperidin-4-yl)oxy)-1,3-dimethyl-1H-purine-2,6(3H,7H)-dione, TFA (**54**, 14.7 mg, 0.026 mmol, 43% yield). ¹H NMR (400 MHz, DMSO-*d*₆) δ 5.20 (dt, *J* = 7.4, 3.7 Hz, 1H), 4.04 (t, *J* = 7.0 Hz, 2H), 3.95–3.39 (m, 4H), 3.36 (s, 3H), 3.19 (s, 3H), 2.19–1.45 (m, 12H), 1.25–1.02 (m, 4H), 0.89 (m, 2H), 0.76–0.63 (m, 4H). LC–MS (method 2): *t*_R = 5.99 min, *m/z* (M + H)⁺ = 458. HRMS calculated for C₂₄H₃₆N₅O₄ (M + H)⁺: 458.2762. Found: 458.2772.

Preparation of Ethyl 4-((1,3-Dimethyl-7-(3-methylbenzyl)-2,6-dioxo-2,3,6,7-tetrahydro-1H-purin-8-yl)methyl)piperazine-1-carboxylate (5**).** To 1,3-dimethyl-7-(3-methylbenzyl)-2,6-dioxo-2,3,6,7-tetrahydro-1H-purine-8-carbaldehyde (**25a**, 62.5 mg, 0.2 mmol) was added a solution of ethyl piperazine-1-carboxylate (95 mg, 0.600 mmol) in CH₂Cl₂ (2 mL) at rt. The mixture was stirred for 3–5 min, and sodium triacetoxyborohydride (212 mg, 1.000 mmol) was added. The mixture was stirred at rt for 1.5 h and was poured into CH₂Cl₂/Na₂CO_{3(aq)} (3 mL/3 mL). The aqueous layer was extracted with CH₂Cl₂ (3 mL × 2). The combined organic layer was dried (Na₂SO₄) and filtered. After removal of solvent, the crude product was purified by silica gel chromatography using 50–80% EtOAc/hexane as the eluent to give ethyl 4-((1,3-dimethyl-7-(3-methylbenzyl)-2,6-dioxo-2,3,6,7-tetrahydro-1H-purin-8-yl)methyl)piperazine-1-carboxylate (87 mg, 0.191 mmol, 96% yield). ¹H NMR (400 MHz, chloroform-*d*) δ 7.24–7.15 (m, 1H), 7.12–7.04 (m, 1H), 6.92 (ddd, *J* = 7.6, 1.9, 0.9 Hz, 2H), 5.73 (s, 2H), 4.13 (q, *J* = 7.1 Hz, 2H), 3.59 (s, 3H), 3.54 (s, 2H), 3.41 (s, 7H), 2.39 (t, *J* = 5.2 Hz, 4H), 2.31 (s, 3H), 1.25 (t, *J* = 7.1 Hz, 3H). LC–MS (method 1): *t*_R = 2.80 min, *m/z* (M + H)⁺ = 455.

Preparation of 8-((4-(Cyclopropanecarbonyl)piperazin-1-yl)methyl)-7-isopentyl-1,3-dimethyl-1H-purine-2,6(3H,7H)-dione, HCl (64**).** To a mixture of 7-isopentyl-1,3-dimethyl-2,6-dioxo-2,3,6,7-tetrahydro-1H-purine-8-carbaldehyde (**25g**, 195 mg, 0.7 mmol) and cyclopropyl(piperazin-1-yl)methanone, HCl (267 mg, 1.400 mmol)

were added CH_2Cl_2 (6 mL) and then Et_3N (0.293 mL, 2.100 mmol) at rt. The mixture was stirred for 3–5 min, and sodium triacetoxyborohydride (297 mg, 1.400 mmol) was added. The mixture was stirred at rt for 4 h and was poured into $\text{CH}_2\text{Cl}_2/\text{Na}_2\text{CO}_3(\text{aq})$ (5 mL/5 mL). The aqueous layer was extracted with CH_2Cl_2 (5 mL \times 2). The combined organic layer was dried (Na_2SO_4) and filtered. After removal of solvent, the crude product was purified by silica gel chromatography using 0–5% MeOH/EtOAc as the eluent to give 8-((4-(cyclopropanecarbonyl)piperazin-1-yl)methyl)-7-isopentyl-1,3-dimethyl-1H-purine-2,6(3H,7H)-dione (251 mg, 0.603 mmol, 86% yield). ^1H NMR (400 MHz, $\text{DMSO}-d_6$) δ 4.30 (dd, $J = 9.7, 5.6$ Hz, 2H), 3.70 (s, 2H), 3.63 (s, 2H), 3.43 (s, 2H), 3.39 (s, 3H), 3.21 (s, 3H), 2.41 (m, 4H), 1.93 (m, 1H), 1.68 (m, 3H), 0.94 (d, $J = 5.9$ Hz, 6H), 0.68 (tt, $J = 7.9, 2.9$ Hz, 4H); ^{13}C NMR (101 MHz, chloroform- d) δ 171.91, 154.78, 151.50, 148.67, 147.53, 107.79, 54.48, 53.22, 52.89, 45.14, 44.50, 41.80, 39.73, 29.67, 27.86, 26.15, 22.39, 10.80, 7.40 (four peaks shown on piperazine ring). LC–MS (method 1): $t_{\text{R}} = 2.82$ min, m/z ($M + \text{H}$) $^+ = 417$. HRMS calculated for $\text{C}_{21}\text{H}_{32}\text{N}_6\text{O}_3\text{Na}$ ($M + \text{Na}$) $^+$: 439.2428. Found: 439.2443. This material was converted to its HCl salt for PK study. To a solution of 8-((4-(cyclopropanecarbonyl)piperazin-1-yl)methyl)-7-isopentyl-1,3-dimethyl-1H-purine-2,6(3H,7H)-dione (250 mg, 0.600 mmol) in 1,4-dioxane (6 mL) at rt was added HCl solution (4 M in 1,4-dioxane, 0.3 mL, 1.2 mmol, 2 equiv). The mixture was stirred at rt for 5 min, and hexane (15 mL) was added and stirred for 15 min. The solid was filtered and washed with hexane (5 mL \times 3) and dried in vacuo to give 8-((4-(cyclopropanecarbonyl)piperazin-1-yl)methyl)-7-isopentyl-1,3-dimethyl-1H-purine-2,6(3H,7H)-dione, HCl (64, 270 mg, 0.596 mmol, 99% yield) as a white solid. Mp 187–189 °C; ^1H NMR (400 MHz, $\text{DMSO}-d_6$) δ 4.36 (d, $J = 7.6$ Hz, 2H), 3.55 (s, 2H), 3.43 (s, 3H), 3.23 (s, 3H), 2.07–1.89 (m, 1H), 1.64 (m, 3H), 0.93 (d, $J = 6.2$ Hz, 6H), 0.73 (d, $J = 7.7$ Hz, 4H) (The protons of piperazine ring (8 H) are very broad between 4.6 and 2.8 ppm).

Biological Methods. Protein Expression and Activity Measurement. Human ALDH1A1, ALDH1B1, and ALDH3A1 were expressed and purified as described elsewhere.^{34–36} Human ALDH2 was purchased from Abcam (Cambridge, MA).

General Protocol for ALDH Enzymatic Assays. Briefly, an amount of 3 μL of enzyme (final concentration 20, 50, 20, and 5 nM for ALDH1A1, ALDH1B1, ALDH2, and ALDH3A1, respectively) or assay buffer (100 mM HEPES, pH 7.5, with 0.01% Tween 20) was dispensed into a 1536-well solid-bottom black plate (Greiner Bio One, Monroe, NC) followed by pin-tool transfer (23 nL) of candidate inhibitors (final concentration range 968 pM to 57.2 μM) and control (Bay 11-7085, final concentration range from 1.31 nM to 2.86 μM). Samples were incubated (rt, protected from light) for 15 min followed by a 1 μL substrate addition of NAD^+ and propionaldehyde (final concentrations of 1 mM and 80 μM , respectively, for ALDH1A1, ALDH1B1, and ALDH2; or NAD^+ and benzaldehyde at 1 mM and 200 μM , respectively, for ALDH3A1). Plates were centrifuged at 1000 rpm for 15 s, then read in kinetic mode on a ViewLux high-throughput CCD imager (PerkinElmer) equipped with standard UV fluorescence optics (340 nm excitation, 450 nm emission) for 10 min (ALDH1A1, ALDH1B1, ALDH2) or 4 min (ALDH3A1). The change in fluorescence intensity over the 4 or 10 min reaction period was normalized against no-inhibitor and no-enzyme controls, and the resulting percent inhibition data were fitted for biological activity. Disulfiram was used as internal standard with comparable activity to reported potency.¹⁶

Dehydrogenase Selectivity Assays. The inhibitory activity against dehydrogenases HPGD and HSD17 β 4 were measured according to protocols described previously.³⁰

High-Throughput RLM Measurement. Microsomal stability of test articles was determined in a HTS format with the single time point and in the 96-well plates, and automated sample preparation with Tecan EVO 200 robot and LC/MS/MS (Waters Xevo TQ-S) instrument were used to measure the percentage of compound remaining after incubation. This allows the calculation of the in vitro half-life ($t_{1/2}$). Six standard controls were tested in each run: buspirone and propranolol (for short half-life), loperamide and diclofenac (for

short to medium half-life), and carbamazepine and antipyrine (for long half-life). The assay incubation system consisted of 0.5 mg/mL microsomal protein, 1.0 μM drug concentration, and NADPH regeneration system (containing 0.650 mM NADP^+ , 1.65 mM glucose 6-phosphate, 1.65 mM MgCl_2 , and 0.2 unit/mL G6PDH) in 100 mM phosphate buffer at pH 7.4. The incubation was carried out at 37 °C for 15 min. The reaction was quenched by adding 550 μL of acetonitrile (~1:2 ratio) containing 0.28 μM albendazole (internal standard). After a 20 min centrifugation at 3000 rpm, 30 μL of the supernatant was transferred to an analysis plate and was diluted 5-fold using 1:2 v/v acetonitrile/water before the samples were analyzed by LC/MS–MS.

■ ASSOCIATED CONTENT

📄 Supporting Information

Additional supplemental figures, tables, and detailed experimental procedures and spectroscopic data (^1H NMR, LC–MS, HRMS) for screening compounds; a xlsx file containing molecular formula strings. The Supporting Information is available free of charge on the ACS Publications website at DOI: 10.1021/acs.jmedchem.5b00577.

■ AUTHOR INFORMATION

Corresponding Authors

*S.-M.Y.: e-mail, yangs9@mail.nih.gov; phone, 301-217-4685.

*D.J.M. (for major correspondence and request of material): e-mail, maloneyd@mail.nih.gov; phone, 301-217-4381; fax, 301-217-5736.

Notes

The authors declare no competing financial interest.

■ ACKNOWLEDGMENTS

S.-M.Y., A.Y., M.L.-N., K.N., K.B., A.W., X.X., M.F., A.S., A.J., and D.J.M. were supported the intramural research program of the National Center for Advancing Translational Sciences and the Molecular Libraries Initiative of the National Institutes of Health Roadmap for Medical Research (Grant U54MH084681). The authors thank Sam Michael and Richard Jones for automation support; Paul Shinn, Danielle van Leer, Crystal McKnight, and Misha Itkin for the assistance with compound management; William Leister, Heather Baker, Elizabeth Fernandez, Burchelle Blackman, and Christopher Leclair for analytical chemistry and purification support; and Emma Hughes for preparing plasma samples for bioanalytical characterization. This research was also supported in part by National Institutes of Health Grants AA022057 (V.V.) and AA021724 (V.V.).

■ ABBREVIATIONS USED

ADME, absorption, distribution, metabolism, and excretion; ALDH, aldehyde dehydrogenase; CSC, cancer stem cell; eADME, early absorption, distribution, metabolism, and excretion; HPbCD, hydroxypropyl β -cyclodextrin; HPGD, 15-hydroxyprostaglandin dehydrogenase; HSD17 β 4, type 4 hydroxysteroid dehydrogenase; qHTS, quantitative high throughput screening; RLM, rat liver microsomes; SAR, structure–activity relationship

■ REFERENCES

- (1) Black, W.; Vasiliou, V. The aldehyde dehydrogenase gene superfamily resource center. *Hum. Genomics* **2009**, *4*, 136–142.
- (2) Marchitti, S. A.; Brocker, C.; Stagos, D.; Vasiliou, V. Non-P450 aldehyde oxidizing enzymes: the aldehyde dehydrogenase superfamily. *Expert Opin. Drug Metab. Toxicol.* **2008**, *4*, 697–720.

- (3) Rizzo, W. B.; Carney, G. Sjögren-Larsson syndrome: Diversity of mutations and polymorphisms in the fatty aldehyde dehydrogenase gene (ALDH3A2). *Hum. Mutat.* **2005**, *26*, 1–10.
- (4) Marchitti, S. A.; Deitrich, R. A.; Vasiliou, V. Neurotoxicity and metabolism of the catecholamine-derived 3,4-dihydroxyphenylacetaldehyde and 3,4-dihydroxyphenylglycolaldehyde: The role of aldehyde dehydrogenase. *Pharmacol. Rev.* **2007**, *59*, 125–150.
- (5) Smith, C.; Gasparetto, M.; Jordan, C.; Pollyea, D. A.; Vasiliou, V. The effects of alcohol and aldehyde dehydrogenases on disorders of hematopoiesis. *Adv. Exp. Med. Biol.* **2015**, *815*, 349–359.
- (6) Ma, I.; Allan, A. L. The role of human aldehyde dehydrogenase in normal and cancer stem cells. *Stem Cell Rev. Rep.* **2011**, *7*, 292–306.
- (7) Tanei, T.; Morimoto, K.; Shimazu, K.; Kim, S. J.; Tanji, Y.; Taguchi, T.; Tamaki, Y.; Noguchi, S. Association of breast cancer stem cells identified by aldehyde dehydrogenase 1 expression with resistance to sequential Paclitaxel and epirubicin-based chemotherapy for breast cancers. *Clin. Cancer Res.* **2009**, *15*, 4234–4241.
- (8) Vasiliou, V.; Thompson, D. C.; Smith, C.; Fujita, M.; Chen, Y. Aldehyde dehydrogenases: From eye crystallins to metabolic disease and cancer stem cells. *Chem.-Biol. Interact.* **2013**, *202*, 2–10 and references cited therein.
- (9) Yue, L.; Huang, Z.-M.; Fong, S.; Leong, S.; Jakowatz, J. G.; Charruyer-Reinwald, A.; Wei, M.; Ghadially, R. Targeting ALDH1 to decrease tumorigenicity, growth and metastasis of human melanoma. *Melanoma Res.* **2015**, *25*, 138–148.
- (10) Luo, Y.; Dallaglio, K.; Chen, Y.; Robinson, W. A.; Robinson, S. E.; McCarter, M. D.; Wang, J.; Gonzalez, R.; Thompson, D. C.; Norris, D. A.; Roop, D. R.; Vasiliou, V.; Fujita, M. ALDH1A isozymes are markers of human melanoma stem cells and potential therapeutic targets. *Stem Cells* **2012**, *30*, 2100–2113.
- (11) Kiefer, F. W.; Orasanu, G.; Nallamshetty, S.; Brown, J. D.; Wang, H.; Luger, P.; Qi, N. R.; Burant, C. F.; Duester, G.; Plutzky, J. Retinaldehyde dehydrogenase 1 coordinates hepatic gluconeogenesis and lipid metabolism. *Endocrinology* **2012**, *153*, 3089–3099.
- (12) Kiefer, F. W.; Vernochet, C.; O'Brien, P.; Spoerl, S.; Brown, J. D.; Nallamshetty, S.; Zeyda, M.; Stulnig, T. M.; Cohen, D. E.; Kahn, C. R.; Plutzky, J. Retinaldehyde dehydrogenase 1 regulates a thermogenic program in white adipose tissue. *Nat. Med.* **2012**, *18*, 918–925.
- (13) Sanders, T. J.; McCarthy, N. E.; Giles, E. M.; Davidson, K. L.; Haltall, M. L.; Hazell, S.; Lindsay, J. O.; Stagg, A. J. (2014). Increased production of retinoic acid by intestinal macrophages contributes to their inflammatory phenotype in patients with Crohn's disease. *Gastroenterology* **2014**, *146*, 1278–1288.
- (14) Moreb, J. S. Aldehyde dehydrogenase as a marker for stem cells. *Curr. Stem Cell Res. Ther.* **2008**, *3*, 237–246.
- (15) Marcato, P.; Dean, C. A.; Giacomantonio, C. A.; Lee, P. W. K. Aldehyde dehydrogenase: Its role as a cancer stem cell marker comes down to the specific isoform. *Cell Cycle* **2011**, *10*, 1378–1384.
- (16) Koppaka, V.; Thompson, D. C.; Chen, Y.; Ellermann, M.; Nicolaou, K. C.; Juvonen, R. O.; Petersen, D.; Deitrich, R. A.; Hurley, T. D.; Vasiliou, V. Aldehyde dehydrogenase inhibitors: a comprehensive review of the pharmacology, mechanism of action, substrate specificity, and clinical application. *Pharmacol. Rev.* **2012**, *64*, 520–539.
- (17) Arolfo, M. P.; Overstreet, D. H.; Yao, L.; Fan, P.; Lawrence, A. J.; Tao, G.; Keung, W.-M.; Vallee, B. L.; Olive, M. F.; Gass, J. T.; Rubin, E.; Anni, H.; Hodge, C. W.; Besheer, J.; Zablocki, J.; Leung, K.; Blackburn, B. K.; Lange, L. G.; Diamond, I. Suppression of heavy drinking and alcohol seeking by a selective ALDH-2 inhibitor. *Alcohol: Clin. Exp. Res.* **2009**, *33*, 1935–1944.
- (18) Lowe, E. D.; Gao, G.-Y.; Johnson, L. N.; Keung, W. M. Structure of daidzin, a naturally occurring anti-alcohol-addiction agent, in complex with human mitochondrial aldehyde dehydrogenase. *J. Med. Chem.* **2008**, *51*, 4482–4487.
- (19) Keung, W. M.; Vallee, B. L. Daidzin: a potent, selective inhibitor of human mitochondrial aldehyde dehydrogenase. *Proc. Natl. Acad. Sci. U. S. A.* **1993**, *90*, 1247–1251.
- (20) Yao, L.; Fan, P.; Arolfo, M.; Jiang, Z.; Olive, M. F.; Zablocki, J.; Sun, H.-L.; Chu, N.; Lee, J.; Kim, H.-Y.; Leung, K.; Shryock, J.; Blackburn, B.; Diamond, I. Inhibition of aldehyde dehydrogenase-2 suppresses cocaine seeking by generating THP, a cocaine use-dependent inhibitor of dopamine synthesis. *Nat. Med.* **2010**, *16*, 1024–1028.
- (21) Kimble-Hill, A. C.; Parajuli, B.; Chen, C.-H.; Mochly-Rosen, D.; Hurley, T. D. Development of selective inhibitors for aldehyde dehydrogenases based on substituted indole-2,3-diones. *J. Med. Chem.* **2014**, *57*, 714–722.
- (22) Condello, S.; Morgan, C. A.; Nagdas, S.; Cao, L.; Turek, J.; Hurley, T. D.; Matei, D. β -Catenin-regulated ALDH1A1 is a target in ovarian cancer spheroids. *Oncogene* **2015**, *34*, 2297–2308.
- (23) Inglese, J.; Auld, D. S.; Jadhav, A.; Johnson, R. L.; Simeonov, A.; Yasgar, A.; Zheng, W.; Austin, C. P. Quantitative high-throughput screening: A titration-based approach that efficiently identifies biological activities in large chemical libraries. *Proc. Natl. Acad. Sci. U. S. A.* **2006**, *103*, 11473–11478.
- (24) A library of 220 402 compounds was screened at 7 concentrations against hALDH1A1. Inhibition of ALDH1A1 activity was screened by utilizing propionaldehyde as substrate and NAD⁺ as cofactor. An increase in the fluorescence intensity due to conversion of NAD⁺ to NADH was used to measure the enzyme activity. The screening and follow-up results were deposited in PubChem in January, 2008 (PubChem bioassay identifier AID 1030 and AID 493210; compound identifier CID 667135 for **5** and CID 3596188 for **6**).
- (25) Notably, indolinedione appeared to be one of active chemotypes in our qHTS screening.
- (26) During the preparation of this manuscript, Hurley reported a high-throughput screening that indicated the theophylline core is one of the active chemical series inhibiting ALDH1A1; see the following: Morgan, C. A.; Hurley, T. D. Development of a high-throughput in vitro assay to identify selective inhibitors for human ALDH1A1. *Chem.-Biol. Interact.* **2015**, *234*, 29–37.
- (27) Morgan, C. A.; Hurley, T. D. Characterization of two distinct structural classes of selective aldehyde dehydrogenase 1A1 inhibitors. *J. Med. Chem.* **2015**, *58*, 1964–1975.
- (28) Detailed synthetic procedures for all analogs are provided in [Supporting Information](#).
- (29) Rybár, A.; Antoš, K. 1,3,7-Trisubstituted 8-isothiocyanatomethylxanthines. *Collect. Czech. Chem. Commun.* **1970**, *35*, 1415–1433.
- (30) Duveau, D. Y.; Yasgar, A.; Wang, Y.; Hu, X.; Kouznetsova, J.; Brimacombe, K. R.; Jadhav, A.; Simeonov, A.; Thomas, C. J.; Maloney, D. J. Structure-activity relationship studies and biological characterization of human NAD⁺-dependent 15-hydroxyprostaglandin dehydrogenase inhibitors. *Bioorg. Med. Chem. Lett.* **2014**, *24*, 630–635.
- (31) The multipoint rat liver microsomal stability and human liver microsomal stability (HLM) of **64** are 84 min and >120 min, respectively. Additionally, the HLM of selective analogs **58**, **59**, **61**, **62**, **65**, and **66** is 94, 57, 44, 47, 57, and 66 min, respectively.
- (32) Alnouti, Y.; Klaassen, C. D. Tissue distribution, ontogeny, and regulation of aldehyde dehydrogenase (Aldh) enzymes mRNA by prototypical microsomal enzyme inducers in mice. *Toxicol. Sci.* **2008**, *101*, 51–64.
- (33) Singh, S.; Arcaroli, J.; Chen, Y.; Thompson, D. C.; Messersmith, W.; Jimeno, A.; Vasiliou, V. ALDH1B1 is crucial for colon tumorigenesis by modulating Wnt/ β -catenin, Notch and PI3K/Akt signaling pathways. *PLoS One* **2015**, *10*, e0121648.
- (34) Xiao, T.; Shoeb, M.; Siddiqui, M. S.; Zhang, M.; Ramana, K. V.; Srivastava, S. K.; Vasiliou, V.; Ansari, N. H. Molecular cloning and oxidative modification of human lens ALDH1A1: implication in impaired detoxification of lipid aldehydes. *J. Toxicol. Environ. Health, Part A* **2009**, *72*, 577–584.
- (35) Stagos, D.; Chen, Y.; Brocker, C.; Donald, E.; Jackson, B. C.; Orlicky, D. J.; Thompson, D. C.; Vasiliou, V. Aldehyde dehydrogenase 1B1: Molecular cloning and characterization of a novel mitochondrial acetaldehyde-metabolizing enzyme. *Drug Metab. Dispos.* **2010**, *38*, 1679–1687.
- (36) Pappa, A.; Estey, T.; Manzer, R.; Brown, D.; Vasiliou, V. Human aldehyde dehydrogenase 3A1 (ALDH3A1): biochemical character-

ization and immunohistochemical localization in the cornea. *Biochem. J.* **2003**, *376*, 615–623.